ACTA MECHANICA SINICA, Vol.11, No.1, February 1995 ISSN 0567-7718
Science Press, Beijing, China
Allerton Press, INC., New York, U.S.A.

MOLECULAR DYNAMICS SIMULATION OF CRACK-TIP PROCESSES IN COPPER*

Zhang Yongwei (张永伟) Wang Tzuchiang (王自强) Tang Qiheng (汤奇恒)
(*LNM, Institute of Mechanics, Chinese Academy of Sciences, Beijing* 100080, *China*)

ABSTRACT: The crack tip processes in copper under mode II loading have been simulated by a molecular dynamics method. The nucleation, emission, dislocation free zone (DFZ) and pile-up of the dislocations are analyzed by using a suitable atom lattice configuration and Finnis & Sinclair potential. The simulated results show that the dislocation emitted always exhibits a dissociated fashion. The stress intensity factor for dislocation nucleation, DFZ and dissociated width of partial dislocations are strongly dependent on the loading rate. The stress distributions are in agreement with the elasticity solution before the dislocation emission, but are not in agreement after the emission. The dislocation can move at subsonic wave speed (less than the shear wave speed) or at transonic speed (greater than the shear wave speed but less than the longitudinal wave speed), but at the longitudinal wave speed the atom lattice breaks down.

KEY WORDS: molecular dynamics, crack tip, dislocation, loading rate

I. INTRODUCTION

In the study of fracture of crystal solids, the dislocation nucleation from the crack tip remains an important problem requiring further insight[1−4]. Rice and Thomson[2] used linear elasticity to establish the criterion of nucleation of a discrete dislocation and the transition of ductile and brittle fracture. More recently, Rice[3] used Peierls concept to reanalyze the dislocation nucleation from a crack tip and proposed a new solid state parameter γ_{us}, the unstable stacking energy, to evaluate the critical external loading which corresponds to the dislocation nucleation. The above analysis was unsatisfactory because of its use of the continuum elasticity for crack tip stress field. When a dislocation is very near the crack tip where the nonlinear and atomic lattice effects are great, the atomic force law needs to be considered.

Using the Embedded-Atom Method (EAM)[5] , Baskes, Daw and Foiles[6] investigated the dislocation mobility in nickel. Tan and Yang[7,8] used EAM to calculate the nucleation and emission of dislocations at and near crack tip. Cheung, Argon and Yip[9] also used EAM to analyze the dislocation nucleation from crack tips in α-iron.

Here we use the "N-body" potential proposed by Finnis and Sinclair[10] and constructed by Ackland, Tichy, Vitek and Finnis[11] to simulate the crack tip processes in the ground

Received August 15 1994
* The project supported by the National Natural Science Foundation of China

state. The simulated results give us some comprehensive understandings about the crack tip processes.

II. CALCULATION PROCEDURE

1. Interatomic potential

The interatomic potential used here is the "N-body" potential proposed by Finnis and Sinclair. The equation they used is

$$E_{\text{tot}} = -\sum_i \rho_i^{1/2} + \frac{1}{2}\sum_i \sum_{i(i\neq j)} V_{ij} \tag{1}$$

ρ_i is the second moment of the density of states, and

$$\rho_i = \sum_{j(i\neq j)} \Phi_{ij} \tag{2}$$

V_{ij} and Φ_{ij} are functions depending only on the interatomic distance, and can be obtained by assuming some function forms and then fitting with the experimental data.

2. Method of solution

The mode II isotropic elastic displacement field is used to prescribe the displacement of the border discrete atoms. The loading rate $\dot{K}_{II}$ is used as the loading control parameter. The inner atoms follow the law of Newton

$$\boldsymbol{F}_i = -\frac{\partial \boldsymbol{U}_{\text{tot}}}{\partial \boldsymbol{r}_i} = m_i \cdot \boldsymbol{a}_i \tag{3}$$

In the present paper, the Leapfrog Algorithm is used, which provides an update formulation. The time step in the present calculation is taken to be 1.18×10^{-14}s.

The atomic level stress associated with an atom is calculated by using the potential of Finnis and Sinclair

$$\sigma^i_{\alpha\beta} = \frac{1}{2\Omega^i}\left[\sum_j V'(r^{ij}) - \rho_i^{-1/2}\sum_j \Phi'(r^{ij})\right]\frac{r^{ij}_\alpha r^{ij}_\beta}{r^{ij}} \tag{4}$$

3. The atom lattice geometry

The {110}, {111} and {112} crystallographic planes of the parallelepiped with a slit are used in the present calculations. The x, y and z axes of the coordinate system are selected to be along ⟨110⟩, ⟨112⟩ and ⟨111⟩ directions, respectively. In FCC crystal, dislocation moves in ⟨110⟩ direction on {111} plane. So, in the present model as shown in Fig.1, crack plane is taken to be {111} plane, crack front is along ⟨112⟩ direction. Under mode II loading, the dislocations shall move along ⟨110⟩ direction. The periodicity along ⟨111⟩ is 3 layers, along ⟨110⟩ is 2 layers and along ⟨112⟩ is 6 layers. Since a long extension in slip direction is particularly important, here the ⟨110⟩ slip direction is made as extensive as is feasible in the computation.

A full dislocation in copper will be dissociated into two partial dislocations, between the two partial dislocations, there is a faulted plane. As for the periodicity condition is used along ⟨112⟩ direction, the nucleation and motion of partial dislocations can be described with the present lattice configuration.

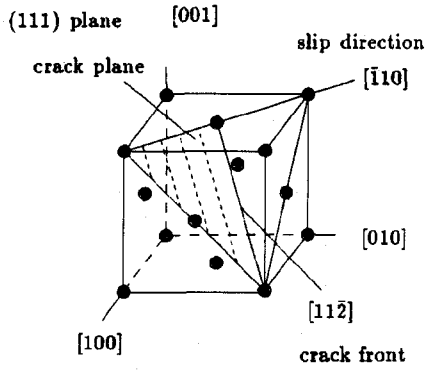

Fig.1 Crack tip and crystallographic geometry in FCC crystal

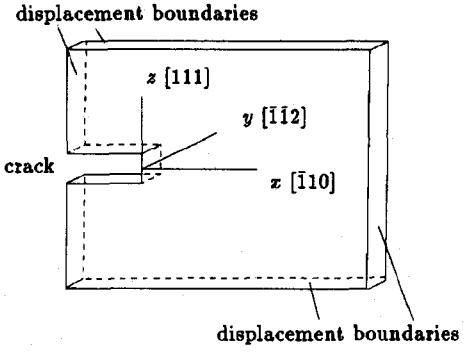

along x: 90 periods, 180 layers
along y: 1 period, 6 layers
along z: 20 periods, 60 layers

Fig.2 The schematic diagram of present calculated model

4. The boundary conditions

The calculated model is schematically shown in Fig.2. The boundary conditions applied to the boundary of the discrete atom region in our molecular dynamics simulation are that of a prescribed displacement distribution dictated by mode II isotropic K field in x-z plane. Along y-direction, a six layer periodic representation is applied. So the present atom lattice is actually three dimensional. The total number of atoms for the simulation is $N = 10760$. The length along x-direction is $\frac{\sqrt{2}}{4} \times 180a_0$ (a_0 is the lattice constant), the width along z-direction $\frac{\sqrt{3}}{3} \times 60a_0$. The distance between the crack tip and the left boundary is $\frac{\sqrt{2}}{4} \times 20a_0$. As the length from the crack tip to the right boundary is large enough, the effect of the boundary constraints on the nucleation and emission of dislocations can be neglected if the dislocations are not too close to the boundary. On the other hand, if we take the boundary as an obstacle to block the moving dislocations, then the pile-up of dislocations can then be set up.

III. RESULTS AND DISCUSSIONS

In the present paper, several cases under different loading rate have been calculated, but here only one of these cases, with the loading rate $\dot{K}_{II} = 0.02034$ MPa$\sqrt{\text{m}}$/ps (1ps = 10^{-12}s), is reported in details. The results obtained from other cases are also reported.

For the case of $\dot{K}_{II} = 0.02034$ MPa$\sqrt{\text{m}}$/ps, the first partial dislocation is nucleated at $K_{II} = 0.33$ MPa$\sqrt{\text{m}}$, and it only takes 0.553ps for this partial dislocation to be accelerated to an approximate constant speed of $v = 1812$ m/s. But at the distance of $11.55a_0$ from the crack tip, the dislocation changes its speed to about 1549 m/s. At $K_{II} = 0.43$ MPa$\sqrt{\text{m}}$, the second partial dislocation is nucleated, it accelerates very quickly to the speed of about 1816 m/s. At the distance of $14.68a_0$, its speed becomes approximately 1460 m/s. All these speeds are below the shear wave speed of 2215 m/s and longitudinal wave speed of 4560 m/s for copper. The separation between two partial dislocations is about 60Å, which is well in

the range predicted by Rice[3]. Figure 3 shows curves between the dislocation positions vs. loading level K_{II}. It can be seen that the separation of the two partial dislocations remains approximately the same except when the first dislocation is blocked by the border. When the first full dislocation is emitted, there exists a DFZ between the crack tip and the full dislocation. Figure 4 shows the atom configuration at $K_{II} = 0.48$ MPa$\sqrt{\text{m}}$. The two partial dislocations can be clearly observed. The shear stresses along the prolongation of the crack plane are shown in Figs.5(a)(b) at the loading levels of $K_{II} = 0.24$ MPa$\sqrt{\text{m}}$ and $K_{II} = 0.48$ MPa$\sqrt{\text{m}}$. The shear stresses of elastic crack tip field and discrete dislocation (the shear stress at dislocation core is corrected by Peierls dislocation) are also plotted on the same figure. The linear elastic solution of interaction field produced by singularity of crack tip and the edge dislocations with Burgers' vector b is

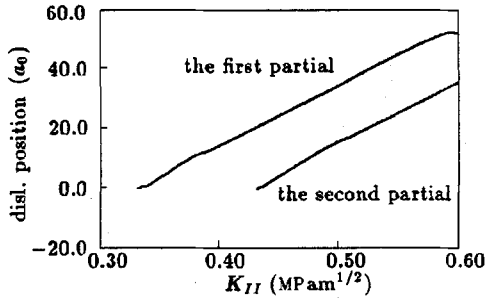

Fig.3 The variations of positions of the partial dislocations with the loading level K_{II}. Two partial dislocations have been emitted

$$\sigma_{xz} = \frac{K_{II}}{\sqrt{2\pi x}} + \sum_i \frac{\mu}{2\pi(1-\nu)} \sqrt{\frac{x_i}{x}} \frac{b}{x - x_i} \tag{5}$$

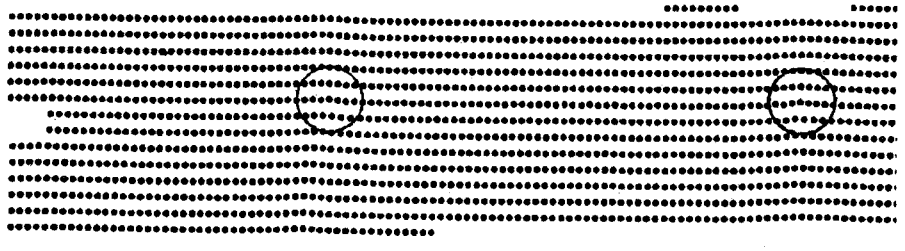

Fig.4 The lattice atoms near the crack tip at $K_{II} = 0.48$ MPa$\sqrt{\text{m}}$. The two partial dislocations can be clearly observed

The stress produced by Eq.(5) ensures traction-free at crack planes. The shear stress very near the dislocation core corrected by Peierls dislocation is

$$\sigma_{xz} = \frac{\mu b}{2\pi(1-\nu)} \frac{x}{x^2 + \zeta^2} \tag{6}$$

It is shown that before the dislocation nucleation, our results are in good agreement with elasticity solution(see Fig.5(a)). After the dislocation emission, our results are in disagreement with elasticity solution(see Fig.5(b)). The stress level of our results is lower than the elasticity solution. This is because the stress of our results does not have singularity at the crack tip and the stress level at the dislocation core is lower than that of the Peierls dislocation due to the relaxation of the atoms at dislocation core.

Our calculations also show that the edge dislocation can not only move at subsonic velocity, but also move at transonic velocity. But at the longitudinal wave speed, the atom lattice breaks down. The results are consistent with that of Weiner and Pear[12].

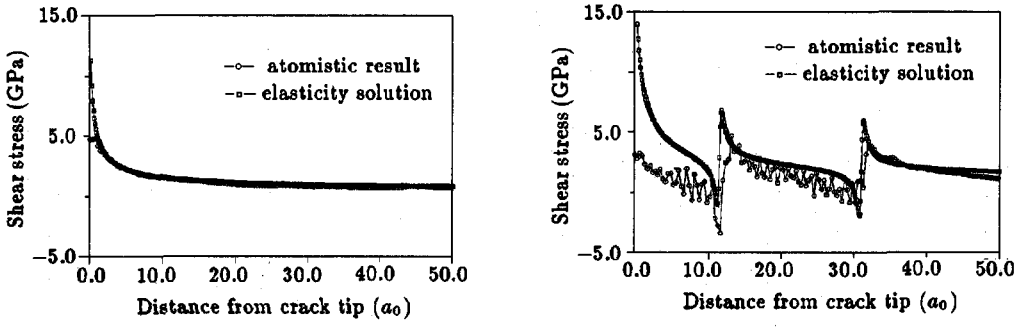

Fig.5 The comparison of atomistic results and elasticity solutions, (a) before dislocation nucleation $K_{II} = 0.24$ MPa$\sqrt{\text{m}}$; (b) after dislocation emission $K_{II} = 0.48$ MPa$\sqrt{\text{m}}$ ($\dot{K}_{II} = 0.02034$ MPa$\sqrt{\text{m}}$/ps)

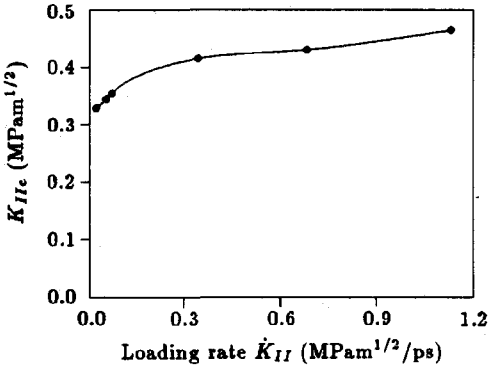

Fig.6 The critical stress intensity factor of the first partial dislocation emission K_{IIe} vs. loading rate $\dot{K}_{II}$

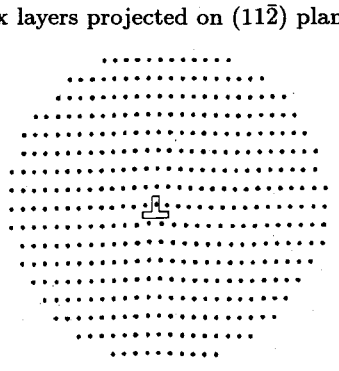

Fig.7 The atom configuration at the dislocation core. The relaxation of atoms can be observed

The relation between the critical stress intensity factor of the first partial dislocation K_{IIe} and loading rate $\dot{K}_{II}$ is shown in Fig.6. We find that K_{IIe} increases with the increase of $\dot{K}_{II}$. We also find that when $\dot{K}_{II} = 1.15$ MPa$\sqrt{\text{m}}$/ps, a partial dislocation is nucleated, but at the same time, the atom lattice breaks down. The speed of the partial dislocation under the loading rate just corresponds to the longitudinal wave speed. The loading rate is the critical loading rate for transition from ductile to brittle.

At higher loading rate, the separations of the partial dislocations and those of full dislocations become very close. We also find that even at lower loading rate, when the pile-up of the dislocations develops at some K_{II}, the atom lattice also breaks down. For example, when the loading rate $\dot{K}_{II} = 0.0638$ MPa$\sqrt{\text{m}}$/ps is applied, atom lattice breaks down at $K_{II} = 1.36$ MPa$\sqrt{\text{m}}$. But at the same loading rate $\dot{K}_{II}$ and loading level K_{II}, the failure does not take place when we enlarge the length along x-direction.

Figure 7 shows the partial dislocation core structure. The core structure is different from that of the discrete dislocation and Peierls dislocation. It can be seen that the relaxation of core atoms takes place due to a high stress level at the dislocation core.

IV. CONCLUSIONS

The present molecular dynamics simulation of crack tip processes can give us several insights and comprehensive understanding of nucleation, emission, DFZ, pile-up of dislocations and the behaviours of moving dislocations.

1. The critical stress intensity factor for the first partial dislocation K_{IIe} is associated with the loading rate, the higher the loading rate, the higher the K_{IIe} will be. For copper, the critical loading rate for transition from ductile to brittle is $\dot{K}_{II} = 1.15$ MPa$\sqrt{\text{m}}$/ps in the present calculation.
2. The stress fields are consistent with the elastic stress field before the dislocation nucleation, but inconsistent with the elastic stress field plus discrete dislocations (stress at dislocation core is corrected by Peierls dislocation field stress) after the dislocation emission, and the dislocation core structure is not the same as the discrete dislocation and Peierls dislocation because of the relaxation of atoms at the dislocation core.
3. For copper, a full dislocation always dissociates into two partial dislocations. The separation of the two partial dislocations depends on the loading rate. The separation of the full dislocations also depends on the loading rate.
4. The dislocation can move at subsonic speed and transonic speed. When dislocation moves at longitudinal wave speed, the atom lattice breaks down, which means that the brittle failure occurs.
5. The present boundary condition can be used to simulate the pile-up of the dislocations. The pile-up of dislocations increases K_{IIe} because of the back stress of the pile-up of dislocations. The brittle failures may occur due to the high K_{IIe}, here the failure exhibits the breakdown of the atom lattice.
6. The size of DFZ depends on the loading rate. The higher the loading rate, the smaller the DFZ size will be.

Acknowledgement: We are grateful to Prof. ZHOU Fuxin and M.Sc. ZHONG Jun for helpful discussions.

REFERENCES

[1] Thomson R. Physics of fracture. *Solid State Phys*, 1986, 39: 1

[2] Rice JR and Thomson R. Ductile versus brittle behaviour of crystals. *Philos Mag*, 1974, 29: 73

[3] Rice JR. Dislocation nucleation from a crack tip: an analysis based on the Peierls concept. *J Mech Phys Solid*, 1992, 40: 239

[4] Ohr SM. An electron microscope study of crack tip deformation and its impact on the dislocation theory of fracture. *Mater Sci Engng*, 1985, 72: 1

[5] Daw MS and Baskes MI. Embedded-atom method: derivation and application to impurities, surfaces, and other defects in metals. *Phys Rev*, B 1984, 29: 6443

[6] Baskes MI, Daw MS and Foiles SM. The embedded atom method: theory and application. *Mat Res Soc Symp Proc*, 1989, 141, 31

[7] Tan HL and Yang W. Atomistic/continuum simulation of interfacial fracture: part I: atomistic simulation. *Acta Mechanica Sinica*, 1994, 10(2): 151

[8] Tan HL and Yang W. Atomistic/continuum simulation of interfacial fracture: part II: atomistic/dislocation/continuum simulation. *Acta Mechanica Sinica*, 1994, 10(3): 237

[9] Cheung KS, Argon AS and Yip S. Activation analysis of dislocation nucleation from crack tip in α-Fe. *J Appl Phys*, 1991, 69: 2088

[10] Finnis MW and Sinclair JE. A simple N-body potential for transition metals. *Philos Mag*, 1984, 50: 45

[11] Ackland GJ, Tichy G, Vitek V and Finnis MW. Simple N-body potentials for noble metals and nickel. *Philos Mag*, A 1987, 56, 735

[12] Weertman J and Weertman JR. Moving dislocations. In: Nabarro FRN, ed. Dislocations in Solids. North-Holland press, 1980, Vol.3